Joseph covariance formula adaptation to Square-Root Sigma-Point Kalman filters

Proceedings of the 5th Jc-IFToMM International Symposium (2022)
The 28th Jc-IFToMM Symposium on Theory of Mechanism and Machines
16th July 2022

A PRELIMINARY SYNTHESIS OF A LIGHT AND COMPACT WEARABLE CABLE-DRIVEN PARALLEL ROBOT FOR WRIST JOINT REHABILITATION

GIOVANNI COLUCCI, ANDREA BOTTA,
MATTIA VERUTTI, CARMEN VISCONTE, GIUSEPPE QUAGLIA
Department of Mechanical and Aerospace Engineering, Politecnico di Torino, Italy,
{ giovanni_colucci; andrea.botta; carmen.visconte; giuseppe.quaglia}@polito.it,
s280289@studenti.polito.it

YING-CHI LIU, YUKIO TAKEDA
Department of Mechanical Engineering, Tokyo Institute of Technology, Japan,
{liu.y.b; takeda.y.aa}@m.titech.ac.jp

ABSTRACT
Robot-assisted rehabilitation has proven to be effective in clinical practice, not only because of its ability to perform repetitive and intensive rehabilitation therapy but also because its rehabilitation outcome is not limited by the lack of experienced therapists or their fatigue due to long and repetitive rehabilitation sessions. Several robotic solutions have been proposed over time, but rarely have these solutions been successful, in particular due to the excessive bulk, discomfort, and joints alignment of the robotic solution. This paper lays the foundation for a preliminary synthesis of a wearable cable-driven parallel robot for wrist joint rehabilitation. Specifically, the synthesis focuses on defining an ad hoc geometric efficiency index to maximise the effective force required to achieve flexion-extension, radial-ulnar deviation and pronation-supination movements with the lowest possible cable tension. To consider lightness and wearability, the results of the synthesis are weighted to obtain a light and compact system that will be developed.

KEY WORDS: Wrist Rehabilitation, Cable-Driven Robot, Parallel Robot, Medical Device, Robot-assisted therapy, Wearable Robot, Mechanism synthesis, SDG 3

1. INTRODUCTION

Clinical studies report that around three-quarters of the working-age population suffer from injuries of varying severity to the upper limbs [1]. Half of these cases are forearm and wrist injuries, while about one-third of bone fractures involve the wrist joint [2]. Frequent and intensive rehabilitation activities enable the recovery of joint mobility after a period of immobility and the ability to recover dexterity in activities of the daily livings (ADLs) [1], [2]. However, such intensive and time-consuming activities highly impact therapists, their lack of numbers, and therefore the recovery outcome. In addition, due to the general ageing of the population, the need for rehabilitation treatment and dedicated staff is expected to increase further.

In this context, robotic rehabilitation has recently gained increasing interest due to the possibility of accurately repeating the movements required for rehabilitation without the direct intervention of the therapist. Many relevant clinical trials based on these robots have been conducted, confirming the effectiveness of robot-assisted rehabilitation [3], [4]. Hussain et al. [5] reported several robotic devices for wrist rehabilitation that have undertaken some experimental evaluations

or clinical trials. The authors divided the robotic devices into two main categories: end-effector and exoskeleton robots. In the first case, the patient's hand grasps the end-effector and is guided in its movements. In the second case, the joints of the robotic device mimic those of the patient, allowing the device to be worn, even if most of the exoskeleton solutions are fixed to the ground.

Although end-effector robots can easily achieve the desired Degrees of Freedom (DoF), the application of accurate forces and torques is complex since their joints do not correspond to those of the patient [5]. On the other hand, exoskeleton robots allow effective exertion of forces due to joint matching, but it is more complex to obtain many DoFs. In this case, special care must be taken that the joints are correctly aligned, otherwise unwanted forces are generated that can damage the joint [6]. Recently, therefore, some solutions have proposed sagging mechanisms to compensate for misalignment [7]–[9]. In addition, both solutions generally use rigid actuators that make the structure rigid, uncomfortable and heavy enough to require it to be attached to a supporting surface [10].

Faced with these critical issues, this paper proposes the preliminary development of a 3 DoF cable-guided end-effector solution that is also wearable, compact, lightweight and requires no external support.

2. CABLE-DRIVEN PARALLEL ROBOT PRELIMINARY DESIGN

2.1 Wrist joint kinematics and requirements

The wrist joint is one of the most complex joints in the upper limbs. It consists of two DoF: (1) the flexion-extension (FE, β) movement about the median-lateral axis, and (2) the radial-ulnar deviation (RUD, γ) movement about the anterior-posterior axis [11]. The respective axes are not fixed but migrate slightly during the movement, therefore the joint would be representable as an ellipsoidal joint. The pronation-supination (PS, α) movement of the entire forearm with respect to the axis passing through the heads of the radius and ulna is also considered among the DoF useful for wrist rehabilitation and ADLs, although it is not an actual DoF of the wrist [11]. Fig.1 depicts a simplified kinematic diagram of the wrist and forearm joints. In particular, the wrist ellipsoidal joint is simplified considering a universal joint between the forearm and the hand whose axes intersect at the wrist centre $\mathbf{O}_W$, while the PS joint is represented as a revolute joint between the elbow and the forearm.

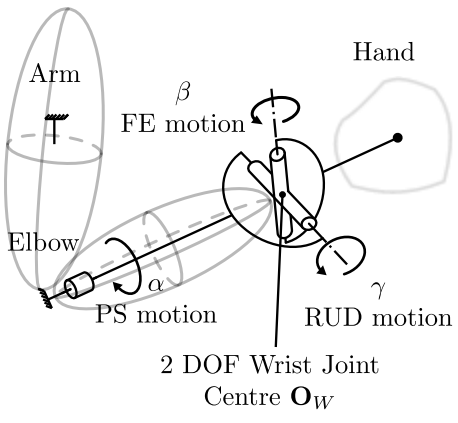

Fig.1 Simplified kinematic diagram of the wrist and forearm joints and their motions

Table 1 Wrist joint maximum and ADLs ranges of motions with the adopted sign convention

Motion	**Max Range**	**ADLs Range**
α, PS pronation $-$ supination $+$	$[-86°, 71°]$	$[-85°, 70°]$
β, FE flexion $+$ extension $-$	$[-71°, 73°]$	$[-54°, 60°]$
γ, RUD radial $+$ ulnar $-$ deviation	$[-33°, 19°]$	$[-33°, 19°]$

There are several studies on the range of motion of the three movements that define both their maximum extension and the range typically required for ADLs [11]–[15]. The various studies differ by a few degrees on the extreme values of the motion ranges, so Table 1 shows the ranges obtained by averaging the values available in the literature.

This paper proposes the synthesis of a robotic rehabilitation device capable of performing PS, FE, and RUD movements in the motion ranges defined in Table 1. Furthermore, the design aims to realise a cable-guided end-effector in order to avoid misalignment with the patient's joints without employing rigid actuators or mechanisms. Finally, it is desired to realise a device that is light, wearable, and comfortable.

2.2 Functional Design

The proposed device comprises two platforms connected to each other by four actuated cables anchored at points $\mathbf{A}_0$, $\mathbf{B}_0$, $\mathbf{A}_1$, and $\mathbf{B}_1$, where 0 indicates the fixed platform and 1 the mobile platform (Fig.2a). The fixed platform (of width $2L_0$ and distance d_0 from $\mathbf{O}_W$) is integral only with the upper part of the arm in order to allow the device to be worn and to correctly distribute the reaction forces over a wide area. The mobile platform (width $2L_1$ and distance d_1 from $\mathbf{O}_W$) is attached to the hand. Between the forearm and the fixed platform there is a revolute joint that allows the PS movement (Fig.2b).

By properly tensioning the 4 cables (the actuation system is integral with the fixed platform) all 3 required DoFs can be achieved. For example, if the cables $\mathbf{P}_1 = \overrightarrow{\mathbf{A}_0\mathbf{A}_1}$ and $\mathbf{P}_2 = \overrightarrow{\mathbf{B}_0\mathbf{A}_1}$ are tensioned more, a radial deviation motion is obtained, vice versa, if the cables $\mathbf{P}_3 = \overrightarrow{\mathbf{A}_0\mathbf{B}_1}$ and $\mathbf{P}_4 = \overrightarrow{\mathbf{B}_0\mathbf{B}_1}$ are tensioned more, an ulnar deviation motion is obtained. Similarly, alternately tensioning pairs $\mathbf{P}_1\mathbf{P}_3$ or $\mathbf{P}_2\mathbf{P}_4$ generates FE motion. Finally, the movement of PS is obtained by acting on the pairs $\mathbf{P}_1\mathbf{P}_4$ or $\mathbf{P}_2\mathbf{P}_3$.

3. CABLE-DRIVEN PARALLEL ROBOT PRELIMINARY SYNTHESIS

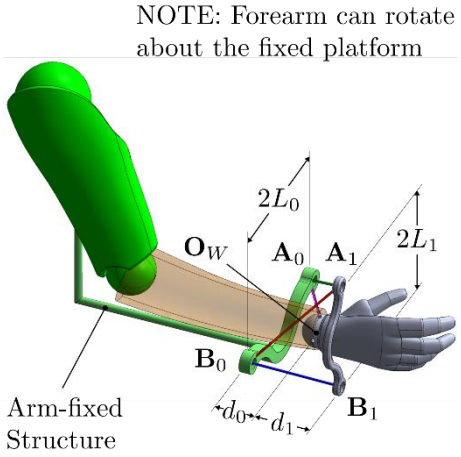

Fig.2a Simplified representation of the cable-driven robot. The fixed platform (green) is fixed to the arm, while the mobile platform (grey) is fixed to the hand (handle not shown). The forearm can rotate about the fixed platform to perform the PS motion

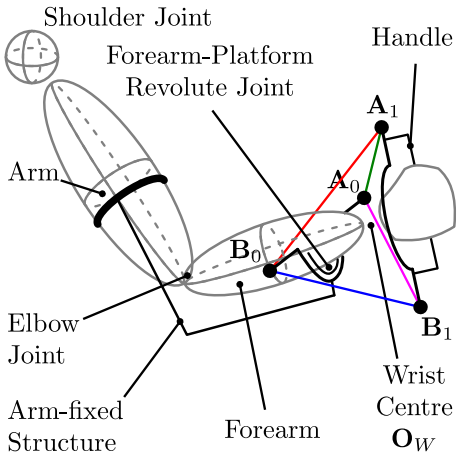

Fig.2b Diagram of the robot working principle. The patient joints are not represented for more clearness. Cable $\mathbf{P}_1$ is green, $\mathbf{P}_2$ is red, $\mathbf{P}_3$ is magenta, and $\mathbf{P}_4$ is blue

3.1 Preliminary Design

A crucial point of cable-driven parallel robots is that the cables must always be in tension to allow proper control of the end-effector (i.e., the mobile platform). In this specific case, this requirement means that there is always an unwanted component of the compressive force of the hand on the wrist. Therefore, it is necessary to accurately size the platforms in order to maximise the force useful to generate the desired movements and at the same time to minimise the axial force that is discharged on the wrist. Nonetheless, it is essential that the overall dimensions are reduced in order to obtain a light and wearable device.

The robot can be sized starting from the size L_j of the platforms and their distance d_j from the wrist centre $\mathbf{O}_W$, where $j = 0, 1$. By correctly designing these parameters it is possible to orient the cables in such a way to minimise the undesired axial force component. In order to perform this design, it is convenient to use non-dimensional parameters to define the proper ratios between the various size regardless of the actual size of the final device. By doing so, it is possible to scale the robot to the desired size maintaining the designed behaviour. In particular, the following dimensionless parameters are defined: $K = L_0/d_1$, $J = L_1/d_1$, and $Q = d_0/d_1$. Respectively, they represent the size of the fixed platform, of the mobile one, and their distance from the centre of the wrist.

3.3 Robot Kinematics and Transmission Index

Before introducing the index used to design the robot, it is useful to define some kinematic relations. Fig.3 illustrates the robot reference frames and its key quantities. $\{\mathbf{O}_j\}$ is the reference frame of the j platform and it is placed at its centre. $\{\mathbf{O}_0\}$ is oriented in such a way that $\boldsymbol{x}_0$ lies along the forearm axis and $\boldsymbol{z}_0$ points toward $\mathbf{B}_0$. $\{\mathbf{O}_1\}$ is defined through a homogeneous transformation in $\{\mathbf{O}_0\}$ composed of a translation of $d_0\boldsymbol{x}_0$, a rotation about the mobile axis with the sequence xyz defined by the angles α, β, γ (the 3 DoF), and then a a translation $d_1\boldsymbol{x}_1$. After that is also possible to define a vector $\mathbf{P}_i$ representing the cable i in the desired referenc frame. Also, it is convenient to define the distance $\mathbf{r}_i$ between the wrist centre $\mathbf{O}_W$ and the anchor point of the i cable onto the mobile platform.

As said before, the design process aims at minimising the reaction force on the wrist along $\boldsymbol{x}_1$ due to cables tension. Thus, it is possible to define a purely geometric transmission index TI_i for each cable. It is defined as the ratio between the projection of $\widehat{\mathbf{P}}_i = \mathbf{P}_i/\|\mathbf{P}_i\|$ along the most effective

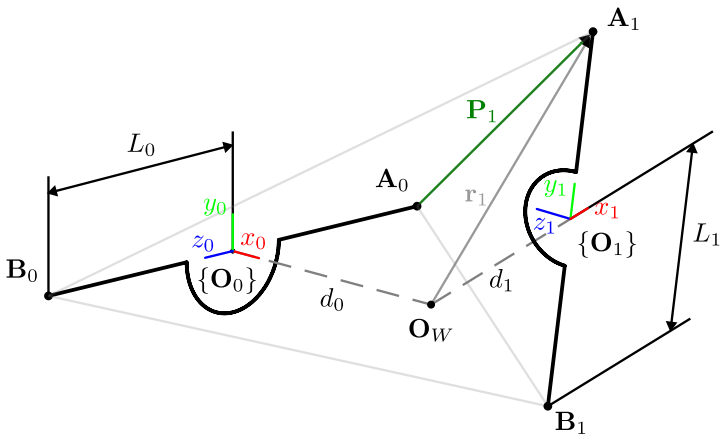

Fig.3 Reference frames and relevant quantities of the rehabilitation device. For clarity, only the vectors relating to cable 1 are shown

direction (i.e., both perpendicular to $\mathbf{r}_i$ and the rotation axis) and the direction of the cable $\widehat{\mathbf{P}}_i$. In other terms

$$\mathrm{TI}_i = \frac{\widehat{\mathbf{P}}_i \cdot (\hat{\mathbf{r}}_i \times \hat{\boldsymbol{a}})}{\widehat{\mathbf{P}}_i} \tag{1}$$

where $\hat{\boldsymbol{a}}$ is the axis of the rotation imposed on the end-effector. A similar approach in defining a transmission index was proposed in [16], in which the most effective direction was introduced for a given output motion, thus the most effective direction was determined once the output motion is defined.

By considering the three elementary motions it is possible to simplify the previous equation. In the case of PS motion, the end-effector rotates about $\boldsymbol{x}_1$, thus the most effective direction is $\boldsymbol{z}_1$ and therefore $\widehat{\mathbf{P}}_i \cdot \boldsymbol{z}_1$ has to be maximised acting on the sizing parameter. Also in the case of FE, when the mobile platform rotates about $\boldsymbol{y}_1$, the component $\widehat{\mathbf{P}}_i \cdot \boldsymbol{z}_1$ is the effective one. In the case of RUD motion, hence a rotation of the end effector about the $\boldsymbol{z}_1$ axis, the effective direction is not parallel to an axis of $\{\mathbf{O}_1\}$ but is a combination of $\boldsymbol{x}_1$ and $\boldsymbol{y}_1$ as function of d_1 and L_1, i.e., the component of $\mathbf{r}_i$. Fig.4 depicts the effective direction for each of the three elementary cases.

3.4 Mechanism Synthesis

In order to know the effects of the parameters K, J, and Q on the 3 DoF and consequently optimise their values to maximise the TI indices, the trend of the TI index of each cable within the desired range of motion was simulated for each elementary movement by varying a single parameter at a time. For the case of RUD, a second alternative condition has also been verified in which α is close to the greater of the extremes of the motion range instead of zero because when $\alpha = 90°$ the TI index reaches the value of 1 around $\gamma = 0°$. Unfortunately, α cannot be 90° because the cables always interfere with the wrist or forearm in this architecture.

Since PS and FE share the same useful direction, the two movements show similar sensitivity to the 3 parameters. In particular, the value of TI increases when the parameter K increases and the parameters J and Q decrease. This means that in order to maximise the TI index for these two movements, the fixed platform should be as large as possible, the mobile platform should be smaller and their distances from the centre of the wrist should be minimal. Regarding the movement of RUD on the contrary, it is observed that large values of Q allow for an increase in the component the

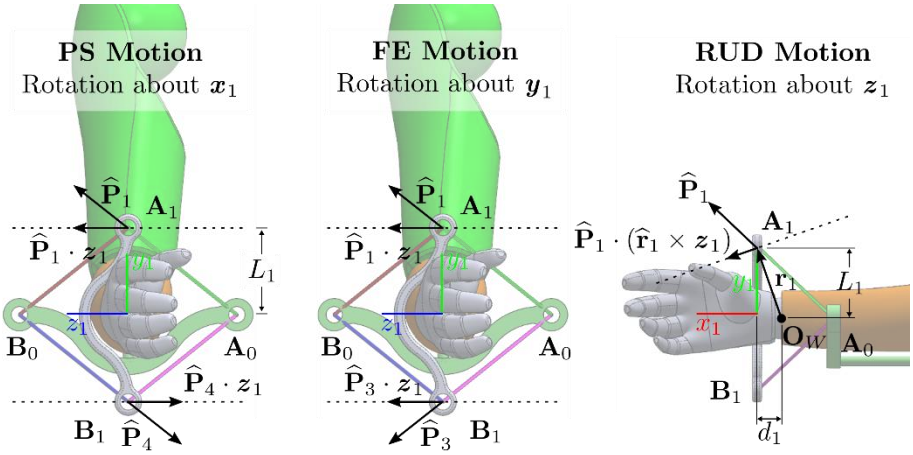

Fig.4 Cable direction and its effective component for each DoF. Both PS and FE motion has $\boldsymbol{z}_1$ as effective direction (but different lever arms), while for the RUD case the effective direction is a function of $\mathbf{r}_i$. Note that $\hat{P}_i$ is the cable direction and not its force vector.

projection of the cable direction along the effective direction, while there are larger values of TI when K and J are similar, particularly if the movement is made with α close to its maximum. Therefore, the resulting robot should have platforms of similar sizes but as far as possible.

However, maximizing TI is not the only target of the synthesis, in fact, lightness and wearability are crucial. To achieve them all 3 parameters K, J, and Q should be as small as possible. Also, the various TI indices should be as constant as possible within the range of motions.

By weighing the various effects, 3 possible device configurations of relatively similar size were identified (Table 2). The first configuration rewards PS and FE movements, while the second is more oriented towards a more effective RUD movement. The third configuration, on the other hand, favours the compactness of the device. Table 3 lists the range of motion for each configuration considering the limitation due to interference verified through a CAD. None of the configurations can achieve the full range of PS motion due to a limit of the proposed architecture (i.e., a cable always interferes with the forearm for a large enough value of α). Nevertheless, the covered ranges should be enough for some rehabilitation exercises regarding the PS motion. Configuration 1 and 2 are able to cover the full range of motions of FE and RUD, sometimes even with large margins. Configuration 3 can perform RUD motion over the full range but has also a limited FE range of motion due to its compact design that leads to interferences between the parts, but it almost covers the respective ADLs range. Fig.5 shows the trend of the transmission index for the various movements and configurations identified.

Table 2 Identified robot configurations. Configuration 1 favours PS and FE motions, Configuration 2 favuors RUD motion, and Configuration 3 favours compactness

Configurations	$L_0[mm]$	$d_0[mm]$	$L_1\ [mm]$	$d_1[mm]$
Configuration 1 K = 8, J = 5, Q = 3	160	60	100	20
Configuration 2 K = 8, J = 5, Q = 3	160	80	100	20
Configuration 3 K = 5, J = 6, Q = 3	100	20	120	60

Table 3 Comparison between DoF range of motion of each configuration and the literature ranges

Configurations	**PS motion [deg]**	**FE motion [deg]**	**RUD motion, $\alpha = 0°$ [deg]**	**RUD motion, $\alpha = \lvert\alpha_{max}\rvert$ [deg]**
Configuration 1 K = 8, J = 5, Q = 3	$[-55°, 55°]$	$[-85°, 85°]$	$[-65°, 65°]$	$[-40°, 40°]$
Configuration 2 K = 8, J = 5, Q = 3	$[-55°, 55°]$	$[-85°, 85°]$	$[-65°, 65°]$	$[-55°, 55°]$
Configuration 3 K = 5, J = 6, Q = 3	$[-55°, 55°]$	$[-57°, 57°]$	$[-70°, 70°]$	$[-30°, 30°]$
Max Range	$[-86°, 71°]$	$[-71°, 73°]$	$[-33°, 19°]$	$[-33°, 19°]$
ADLs Range	$[-85°, 70°]$	$[-54°, 60°]$	$[-33°, 19°]$	$[-33°, 19°]$

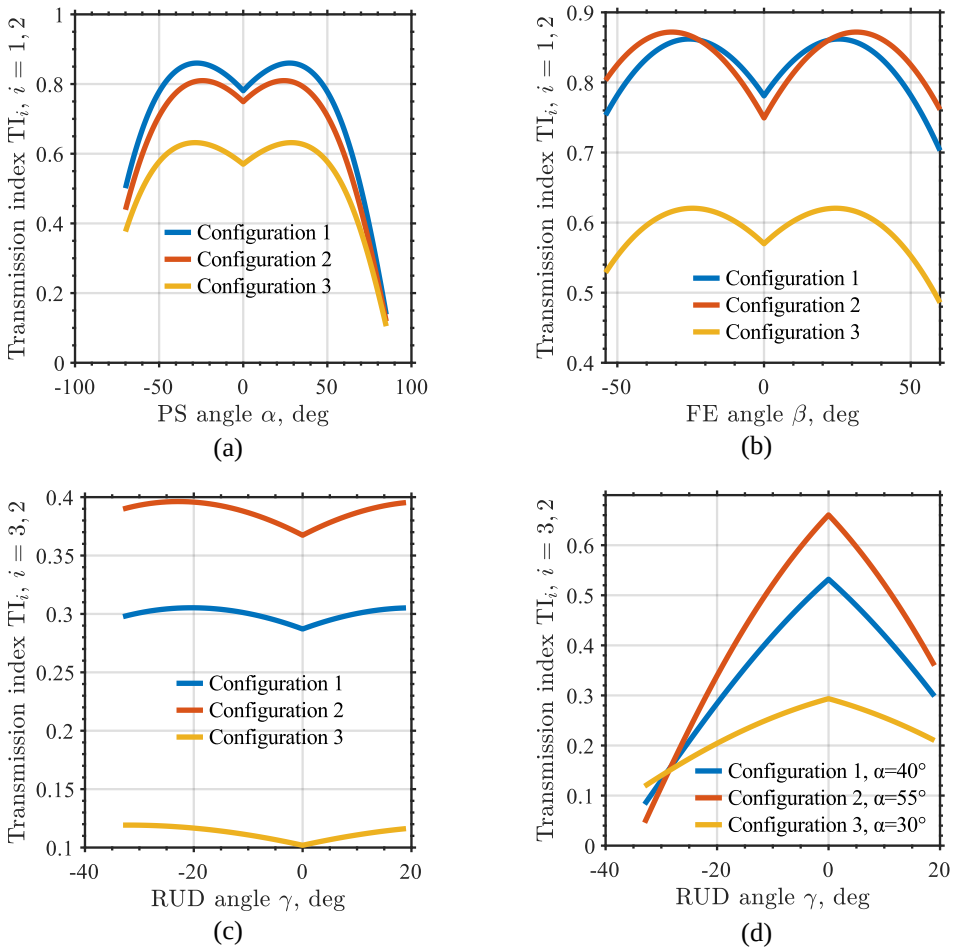

Fig.5 Transmission index TI_i over the range of motion of each DoF for each configuration. (a) PS motion. (b) FE motion. (c) RUD motion with $\alpha = 0°$. (c) RUD motion with $\alpha = |\alpha_{max}|$

4. CONCLUSIONS

This paper has proposed a novel light and compact wearable cable-driven parallel robot for wrist joint rehabilitation with the 3 DoF of the wrist and the forearm. This architecture aims to be a combination of the advantages of end-effector and exoskeleton type devices. This work has focused on the preliminary design of the parallel robot employing a geometric transmission index to optimize its synthesis. After carrying out a sensitivity analysis on the most relevant parameters, 3 promising configurations have been identified. Such configurations will be investigated in order to manufacture an effective prototype.

REFERENCES

[1] C. S. Crowe *et al.*, "Global trends of hand and wrist trauma: a systematic analysis of fracture and digit amputation using the Global Burden of Disease 2017 Study," *Injury Prevention*, vol. 26, no. Suppl 2, pp. i115–i124, Oct. 2020, doi: 10.1136/injuryprev-2019-043495.

[2] G. A. Albanese *et al.*, “Assessment of human wrist rigidity and pain in post-traumatic patients,” in *2019 IEEE 16th International Conference on Rehabilitation Robotics (ICORR)*, Jun. 2019, pp. 89–94. doi: 10.1109/ICORR.2019.8779508.

[3] G. Kwakkel, B. J. Kollen, and H. I. Krebs, “Effects of Robot-Assisted Therapy on Upper Limb Recovery After Stroke: A Systematic Review,” *Neurorehabil Neural Repair*, vol. 22, no. 2, pp. 111–121, Mar. 2008, doi: 10.1177/1545968307305457.

[4] D. J. Reinkensmeyer, L. E. Kahn, M. Averbuch, A. McKenna-Cole, B. D. Schmit, and W. Z. Rymer, “Understanding and treating arm movement impairment after chronic brain injury: progress with the ARM guide.,” *Journal of rehabilitation research and development*, vol. 37, no. 6, pp. 653–662, Nov. 2014.

[5] S. Hussain, P. K. Jamwal, P. Van Vliet, and M. H. Ghayesh, “State-of-the-Art Robotic Devices for Wrist Rehabilitation: Design and Control Aspects,” *IEEE Transactions on Human-Machine Systems*, vol. 50, no. 5, pp. 361–372, Oct. 2020, doi: 10.1109/THMS.2020.2976905.

[6] M. B. Näf, K. Junius, M. Rossini, C. Rodriguez-Guerrero, B. Vanderborght, and D. Lefeber, “Misalignment Compensation for Full Human-Exoskeleton Kinematic Compatibility: State of the Art and Evaluation,” *Applied Mechanics Reviews*, vol. 70, no. 5, Feb. 2019, doi: 10.1115/1.4042523.

[7] Y.-Y. Su, Y.-L. Yu, C.-H. Lin, and C.-C. Lan, “A compact wrist rehabilitation robot with accurate force/stiffness control and misalignment adaptation,” *Int J Intell Robot Appl*, vol. 3, no. 1, pp. 45–58, Mar. 2019, doi: 10.1007/s41315-019-00083-6.

[8] Y.-C. Liu and Y. Takeda, “Kineto-Static Analysis of a Wrist Rehabilitation Robot with Compliance and Passive Joints for Joint Misalignment Compensation,” *Machines*, vol. 8, no. 2, Art. no. 2, Jun. 2020, doi: 10.3390/machines8020023.

[9] Y.-C. Liu, K. Irube, and Y. Takeda, “Kineto-Static Analysis and Design Optimization of a 3-DOF Wrist Rehabilitation Parallel Robot with Consideration of the Effect of the Human Limb,” *Machines*, vol. 9, no. 12, Art. no. 12, Dec. 2021, doi: 10.3390/machines9120323.

[10] M. A. Gull, S. Bai, and T. Bak, “A Review on Design of Upper Limb Exoskeletons,” *Robotics*, vol. 9, no. 1, Art. no. 1, Mar. 2020, doi: 10.3390/robotics9010016.

[11] D. A. Neumann, *Kinesiology of the Musculoskeletal System - Foundations for Rehabilitation*, 3rd ed. Elsevier Health Sciences, 2016.

[12] J. Ryu, W. P. Cooney, L. J. Askew, K.-N. An, and E. Y. S. Chao, “Functional ranges of motion of the wrist joint,” *The Journal of Hand Surgery*, vol. 16, no. 3, pp. 409–419, May 1991, doi: 10.1016/0363-5023(91)90006-W.

[13] G. Brigstocke, A. Hearnden, C. A. Holt, and G. Whatling, “The functional range of movement of the human wrist,” *J Hand Surg Eur Vol*, vol. 38, no. 5, pp. 554–556, Jun. 2013, doi: 10.1177/1753193412458751.

[14] P. M. Kane, B. G. Vopat, C. Got, K. Mansuripur, and E. Akelman, “The Effect of Supination and Pronation on Wrist Range of Motion,” *J Wrist Surg*, vol. 03, no. 3, pp. 187–191, Aug. 2014, doi: 10.1055/s-0034-1384749.

[15] Washington State Department of Social and Health Service, “Range of joint motion evaluation chart.” 2014. [Online]. Available: https://www.dshs.wa.gov/sites/default/files/forms/pdf/13-585a.pdf

[16] Y. Takeda and H. Funabashi, “A Transmission Index for In-Parallel Wire-Driven Mechanisms,” *JSME International Journal Series C Mechanical Systems, Machine Elements and Manufacturing*, vol. 44, no. 1, pp. 180–187, 2001, doi: 10.1299/jsmec.44.180.